



Evaluation of ELF Electric Fields Effects on Bifurcation Phenomenon of Spaced-Clamped Conductance-Based Minimal Cell Models

A.Naghilou^{*1}, S.H.Sabzpoushan²

¹Department of Bioelectric, Science and Technology University, Tehran, Iran

²Department of Bioelectric, Science and Technology University, Tehran, Iran

Received:
29th April 2013
Received in revised form:
20th May 2013
Accepted: 31st May 2013
Available online:
10th June 2013



Online ISSN 2249-622X
<http://www.jbiopharm.com>

ABSTRACT

Spaced clamped Conductance-Based minimal cell models, main basis of more complex neuronal models, e.g. Hodgkin-Huxley model. In this paper, these models have been modified under the influence of ELF electric fields and induced depolarization as a result of such fields is added to the their Nernst potential. By using bifurcation analysis of dynamical systems and considering the injected current and induced voltage as generic parameters of models, the occurrence of dynamical behaviors is justified. Results of this research shows that due to the existence of only an amplifying gating variable and one resonant gating variable in structure of models, bistability phenomenon is caused by Hopf, limit point and LPC (Limit Point Cycle) bifurcations occur and multi-stabilities of higher order than two do not occur. Our simulation results show that the minimal models, $I_{Na,p}+I_h$ and I_h+I_{Kir} , have maximum and minimum dynamical variations, respectively.

Keywords: induced voltage component, Hopf bifurcation, Saddle-node, limit cycle, equilibrium points.

1. INTRODUCTION

Due to the importance of neuronal electrical activities, Hodgkin and Huxley (HH) published a series of their basic papers in 1952 and represented a mathematical model that still serve as a landmark for neuroscience and membrane excitability nowadays [1]. After Hodgkin and Huxley, various types of ionic channels have been discovered and their open-close characteristics have been identified for diverse neuronal membranes. Their electrical excitations have been modeled under the HH formalism [2]. The space-clamped Hodgkin and Huxley equations for the nerve impulse are a system of four nonlinear ordinary differential equations that relate the difference of electric potential across the cell membrane to the membrane's permeability to Na^+ and K^+ ions as a response to an externally applied current stimulus [3].

The dynamics of even one single neuron can be quite complicated. There is always interested in developing techniques to study networks consisting of possibly a large number of coupled neurons. If each single neuron represents complex dynamical behaviors, clearly the

analysis of a network of neurons may be extremely challenging. For this reason, often it is considering simpler, minimal models for single neurons. The insights we can gain from analyzing the minimal models are often more useful in studying the behavior of more complex cell models [4].

Eugene M. Izhikevich suggested that any space-clamped conductance-based model of a neuron either is a minimal model or could be reduced to a minimal space-clamped conductance-based model or models by removing gating variables [5]. A minimal or irreducible model of electrophysiological mechanisms in neurons for spiking must satisfy the following two properties:

- 1) It has a limit cycle attractor, at least for some values of parameters.
- 2) If one removes any current or gating variable, the model has only equilibrium attractors for any values of parameters.

In the structure of a minimal model, a fast positive feedback with a slower negative feedback is used. Gating

variables may be amplifying (positive feedback) or resonant (negative feedback) depending on whether they represent activation/inactivation of inward/outward currents. Two amplifying and two resonant gating variables produce six different combinations. Actually, if an amplifying gating variable has a slow time constant; it would act more as a low-pass filter in order to do not affect fast oscillations and amplifying only slow oscillations. If a resonant gating variable has a fast time constant, it will act to damp input oscillations and resulting in stability of the equilibrium state. Instead, the resonant variable acts as a band-pass filter; it has no effect on oscillations with a period much smaller than its time constant; it damps oscillations having a period much larger than its time constant, because the variable oscillates in phase with the voltage oscillations; it amplifies oscillations with a period that is about the same as its time constant because the variable lags the voltage oscillations [5].

So far, the original HH equations and various kinds of HH-type equations have been analyzed numerically and/or analytically [6]. On the other hand, an exposure of a cell to an external electric field results in the induced transmembrane voltage that superimposes to the resting voltage. This can have a range of effects, from modification of the activity of voltage-gated channels to membrane electroporation [7]. Unlike the resting transmembrane voltage, which is always present and constant everywhere on the plasma membrane, induced voltage component only lasts for the duration of the exposure and varies with the position on the membrane. Consequently, it is often important to accurately determine how electric fields affect the dynamics of neural activity cell models.

The main purpose of the present article is to illustrate how the extremely low frequency (ELF) electric fields affect the dynamics of neural activity in context of minimal space-clamped conductance-based cell equations. The generation mechanism underlying a variety of APs in modified minimal cell equations is explored. In fact, we are going to understand that could the ELF electrical fields in minimal models create multi-stability more than order two similar to the Hodgkin-Huxley model?

2. Methods

2.1 Spaced Clamped Conductance-Based Minimal Neurons Models

According to Fig1, two amplifying and two resonant gating variables produce six different minimal models.

2.1-1 I_{Na,p}+I_K model

Differential equations of the model that consists of a fast Na⁺ current and a relatively slower K⁺ current are as follows:

$$C\dot{v} = I_{ext} - g_L(v - E_L) - g_{Na}m(v - E_{Na}) - g_Kn(v - E_K) \quad (1)$$

$$\dot{m} = \frac{m_{\infty}(v) - m}{\tau_m(v)} \quad (2)$$

$$\dot{n} = \frac{n_{\infty}(v) - n}{\tau_n(v)} \quad (3)$$

		resonant gating variables	
		inactivation of inward current	activation of outward current
amplifying gating variables	activation of inward current	I _{Na,t} -model	I _{Na,p} +I _K -model
	inactivation of outward current	I _{Na,p} +I _h -model	I _A -model I _{Kir} +I _K -model

Fig 1. Any combination of one amplifying variable and one resonant gating variable result in a spiking model [5].

2.1.2 I_{Na,t} model

This model consists of Ohmic leak current and a transient voltage-gated inward Na⁺ current as follows:

$$C\dot{v} = I_{ext} - g_L(v - E_L) - g_{Na}m^3h(v - E_{Na}) \quad (4)$$

$$\dot{m} = \frac{m_{\infty}(v) - m}{\tau_m(v)} \quad (5)$$

$$\dot{h} = \frac{h_{\infty}(v) - h}{\tau_h(v)} \quad (6)$$

2.1.3 I_{Na,p}+I_h model

It consists of one amplifying (I_{Na,p}) and one resonant (I_h) current as follows:

$$C\dot{v} = I_{ext} - g_L(v - E_L) - g_{Na}m(v - E_{Na}) - g_hh(v - E_h) \quad (7)$$

$$\dot{m} = \frac{m_{\infty}(v) - m}{\tau_m(v)} \quad (8)$$

$$\dot{h} = \frac{h_{\infty}(v) - h}{\tau_h(v)} \quad (9)$$

2.1.4 I_h+I_{Kir} model

The I_h+I_{Kir} neuron model for describing a variety of sustained sub-threshold oscillatory voltage patterns is described by:

$$C\dot{v} = I_{ext} - g_L(v - E_L) - g_{Kir}h_{Kir}(v - E_K) - g_hh(v - E_h) \quad (10)$$

$$\dot{h} = \frac{h_{\infty}(v) - h}{\tau_h(v)} \quad (11)$$

$$\dot{h}_{Kir} = \frac{h_{Kir,\infty}(v) - h_{Kir}}{\tau_{Kir}(v)} \quad (12)$$

2.1.5 I_K+I_{Kir} model

The I_K+I_{Kir} comprise the following differential equations:

$$C\dot{v} = I_{ext} - g_{Kir}h(v - E_K) - g_Kn(v - E_K) \quad (13)$$

$$\dot{n} = \frac{n_{\infty}(v) - n}{\tau_n(v)} \quad (14)$$

$$\dot{h} = \frac{h_{\infty}(v) - h}{\tau_h(v)} \quad (15)$$

2.1-6 I_A model

The last minimal voltage-gated model has only one transient K⁺ current, often referred to as the A-current I_A, yet it can also generate sustained oscillatory voltage patterns. The I_A model (pronounced transient potassium model or A-current model) has the form

$$C\dot{v} = I_{ext} - g_L(v - E_L) - g_A m h (v - E_K) \quad (16)$$

$$\dot{m} = \frac{m_{\infty}(v) - m}{\tau_m(v)} \quad (17)$$

$$\dot{h} = \frac{h_{\infty}(v) - h}{\tau_h(v)} \quad (18)$$

In equations (1) to (18), v represents the membrane potential. C is the membrane capacity. While $0 \leq m \leq 1$ and $0 \leq n \leq 1$ are the gating variables that represents activation of the ionic channels. Where $0 \leq h \leq 1$ and $0 \leq h_{Kir} \leq 1$ are the gating variables that represents inactivation of the ionic currents. I_{ext} is the externally applied DC current that is assumed to be temporally constant as a generic parameter and t denotes the time measured in milliseconds. g_A, g_{Na}, g_K, g_{Kir}, g_h and g_L denotes the maximum conductance of corresponding ionic currents. E_{Na}, E_K, E_h, and E_L represent Nernst potentials of Na⁺, K⁺, h-current, and leakage currents, respectively. Also the steady state activation or inactivation X_∞(v) is a voltage-dependent Boltzmann function as follows:

$$X_{\infty}(v)|_{X=m,h,n,h_{Kir}} = \frac{1}{1 + \exp\left(\frac{v_{1/2} - v}{K}\right)} \quad (19)$$

Where v_{1/2} is the activation or inactivation midpoint potential. K denotes the slope factor of the activation or inactivation. Voltage sensitive time constant τ_X(v) is described by the below Gaussian function

$$\tau_X(v)|_{X=m,h,n,h_{Kir}} = C_{base} + C_{amp} \exp\left(\frac{-(v_{max} - v)^2}{\sigma^2}\right) \quad (20)$$

The graph of the function is above C_{base} with amplitude C_{amp}. The maximal value is achieved at v_{max}. The parameter σ measures characteristic width of the graph, i.e.

$$\tau_X(v_{max} \pm \sigma)|_{X=m,h,n,h_{Kir}} = C_{base} + C_{amp}/e.$$

2.2 The modified minimal neuron models exposed to ELF electric field

In exposures of cells to a homogeneous ELF electric field, neuron models is modified[8].The new parameter vE, reflecting the effect of the ELF electric field, as an electromotive force is added to the membrane[8].induced transmembrane potential vE can be calculated as given in[9]. Because, time constant of induced voltage in real biological cells is of the order of 10⁻⁷ and is very small compared with the pulse width of ELF electric fields [9] , it can be considered time independent. Therefore vE does not change the basic structure of minimal models but simultaneously change the Nernst potentials of sodium current, potassium current, A current, h current, and leak

current. Thus the original I_{Na,p}+I_K minimal model is modified as the following form:

$$C\dot{v} = I_{ext} - g_L(v + vE - E_L) - g_{Na}m(v + vE - E_{Na}) - g_Kn(v + vE - E_K) \quad (21)$$

$$\dot{m} = \frac{m_{\infty}(v) - m}{\tau_m(v)} \quad (22)$$

$$\dot{n} = \frac{n_{\infty}(v) - n}{\tau_n(v)} \quad (23)$$

$$m_{\infty}(v) = \frac{1}{1 + \exp\left(\frac{v_{1/2,m} - v}{K_m}\right)} \quad (24)$$

$$n_{\infty}(v) = \frac{1}{1 + \exp\left(\frac{v_{1/2,n} - v}{K_n}\right)} \quad (25)$$

$$\tau_m(v) = C_{base,m} + C_{amp,m} \exp\left(\frac{-(v_{max,m} - v)^2}{\sigma_m^2}\right) \quad (26)$$

$$\tau_n(v) = C_{base,n} + C_{amp,n} \exp\left(\frac{-(v_{max,n} - v)^2}{\sigma_n^2}\right) \quad (27)$$

Other models are modified in the same way. In this paper, we treat I_{ext} and vE as main control parameters, and analyze one-parameter bifurcations and two-parameter bifurcations in the parameter plane of (I_{ext}-vE). The parameter values in Equations of models except for I_{ext} and vE are listed in tables 1, 2 [5].

Model	Current	Maximal Conductance	Nernst Potential
I _{Na,p} +I _h	I _{Na,p}	0.9mS/cm ²	20mV
	I _h	3mS/cm ²	-43mV
	I _L	1.3mS/cm ²	-80mV
I _{Na,p} +I _K	I _{Na,p}	20mS/cm ²	60mV
	I _K	10mS/cm ²	-90mV
	I _L	8mS/cm ²	-80mV
I _h +I _{Kir}	I _h	0.5mS/cm ²	-43mV
	I _{Kir}	4mS/cm ²	-80mV
	I _L	0.44mS/cm ²	-50mV
I _K +I _{Kir}	I _K	2mS/cm ²	-80mV
	I _{Kir}	20mS/cm ²	-80mV
I _{Na,t}	I _{Na}	15mS/cm ²	60mV
	I _L	1mS/cm ²	-70mV
	I _A	5mS/cm ²	-80mV
I _A	I _L	0.2mS/cm ²	-60mV

Table 1: Fixed main parameters for the minimal models [5].

3. Bifurcations dictionary and their numerical detection

As parameters of a dynamical system are varied qualitative changes in the phase portrait may occur at

special values of the parameters. These changes are called bifurcations [3].

Model	Gating variable	$V_{1/2}$	K	v_{max}	σ	C_{amp}	C_{base}
$I_{Na,p}+I_h$	m	-54	9	-	-	-	0.8
	h	-75	-5.5	-75	15	1000	100
$I_{Na,p}+I_K$	m	-20	15	-	-	-	0
	n	-25	5	-	-	-	1
I_h+I_{Kir}	h_{Kir}	-76	-11	-	-	-	0
	h	-65	-5.5	-75	15	1000	100
I_K+I_{Kir}	h_{Kir}	-80	-12	-	-	-	0
	n	-55	5	-	-	-	5
$I_{Na,t}$	m	-40	15	-38	30	0.46	0.04
	h	-62	-7	-67	20	7.4	1.2
I_A	m	-3	20	-71	60	0.92	0.34
	h	-66	-10	-73	23	50	8

Table 2: Fixed gating parameters for the minimal models [5].

We calculate two-parameter bifurcation diagrams (2BDs) by changing *I_{ext}* ($\mu A/cm^2$) as the abscissa and *vE* (mV) as the ordinate. The parameter planes are divided into regions by bifurcation curves consisting of bifurcation points. The co-dimension of a bifurcation is the minimum dimension of the parameter space in which the bifurcation may occur in a persistent way [2]. In 2BDs, bifurcations of co-dimension one appear as curves, and co-dimension two as points. The following are the types of bifurcations we consider in this study [2-6].

3-1-Co-dimension 1 bifurcations

Limit point (LP) or saddle node (sn):

By changing the parameter value, a pair of equilibrium points are created and or annihilated. At this bifurcation point, the Jacobian matrix of the system equations at the equilibrium point has a zero eigenvalue. The coefficient of the fold normal form is nonzero.

Neutral saddle (NS):

Neutral saddle equilibrium occurs when two real eigenvalues have opposite signs. Orbits diverge from the equilibrium along the eigenvector corresponding to the positive eigenvalue.

Hopf bifurcation:

Hopf bifurcations occur when the complex conjugate eigenvalues simultaneously cross the imaginary axis into the right half plane. By changing the value of a parameter, a periodic orbit appears. When the bifurcated orbit is stable, it is the supercritical Hopf (H^+) bifurcation and the first Lyapunov coefficient is negative. Inversely, when the bifurcated orbit is unstable, it is the subcritical Hopf (H^-) bifurcation and the first Lyapunov coefficient is positive.

Limit point of cycles (LPC):

Two oscillatory orbits, one stable and the other unstable with finite amplitude coalesce and disappear.

3-2-Co-dimension 2 bifurcations

Generalized Hopf (GH) bifurcation: There is degeneracy in the way in which periodic orbits collapse onto an equilibrium point at a Hopf bifurcation. At this bifurcation point, the first Lyapunov coefficient vanishes and the second Lyapunov coefficient is nonzero. On a 2BD, GH (Bautin) locates on the Hopf curve, and at this point, a LPC curve is terminated.

Cusp bifurcation: Three equilibrium points coalesce into one. At the Cusp point there is equilibrium with a simple zero eigenvalue but zero coefficient of the fold normal form.

Bogdanov-Takens (BT) bifurcation:

At each BT point, an equilibrium point undergoes Hopf and limit point bifurcations, simultaneously. The Jacobian matrix has double zero eigenvalues and the two bifurcations occur in the same subspace. On a 2BD, BT locates on the LP (sn) curve, and Hopf bifurcation curve is tangent to the sn curve at this point.

3-3-Numerical Detection

To determine the trajectories and the AP waveforms of the models, we used ODE23 in MATLAB and Cellular Open Resource (COR) software [10]. We provide the bifurcation diagrams of models by means of the software package MATCONT [11].

4-Results

In this section, we show numerical results obtained by the bifurcation analysis and observe a global structure of bifurcations in one dimensional (*vE*) and two dimensional (*I_{ext}*-*vE*) parametric spaces for the minimal models. We illustrate the variations of the single parameter bifurcation diagrams for *vE* with different values of *I_{ext}*. The injected current *I_{ext}* is considered constant in certain values and the bifurcation parameter *vE* is continuously varied.

We look at the Hopf and sn curves and LPC points, in particular, and identify the parameter regions in which the minimal models have the multi-stability of periodic orbits and equilibrium points by using 2BDs and single parameter bifurcation diagrams. At single parameter bifurcation diagrams, the central curve represents the equilibrium points and the upper and lower ones shows the maximum and minimum values of periodic orbits, respectively. The stable and unstable orbits are shown by dashed and dotted curves, respectively. The Fig. 2 gives a global view of the bifurcations structure of the $I_{Na,p}+I_K$ model. The Fig.2 (A-E) show the results for *I_{ext}* =320, 300, -100, -200, and -470 $\mu A/cm^2$, respectively. Also, 2BD of the $I_{Na,p}+I_K$ model in (*I_{ext}*-*vE*) plane is shown in Fig.2 (F). In each diagram, the parameters, except for parameters of the coordinate system, are fixed as values for $I_{Na,p}+I_K$ neuron model as shown in Table1.

For *I_{ext}*=320 $\mu A/cm^2$, as *vE* increases from small values, first a supercritical Hopf bifurcation H^+ 1 occurs. The

generated stable limit cycle at H^+ , finally, is terminated at point H^+ . Between these points, steady state of system is a stable limit cycle. In the values outside these two points, the equilibrium point is the unique stable steady state, and the $I_{Na,P}+I_K$ model behaves as an excitable membrane. For $I_{ext}=300 \mu A/cm^2$, as vE reaches the supercritical Hopf bifurcation H^+ , the equilibrium point changes from stable to unstable. By further increasing vE , a subcritical Hopf bifurcation H^- occurs. The stable periodic orbit is bifurcated from an equilibrium point by the supercritical Hopf bifurcation H^+ at bifurcation point LPC is combined with unstable periodic orbit bifurcated from subcritical Hopf bifurcation H^- and is disappeared. For $I_{ext}=-100 \mu A/cm^2$, as vE start to increase from negative values, a supercritical Hopf bifurcation H^+ occur. As vE increases further, three branches of equilibrium points show a Z-shaped curve is joined by LP1 and LP2 bifurcation. Finally, the generated stable limit cycle at H^+ is terminated at point LP1.

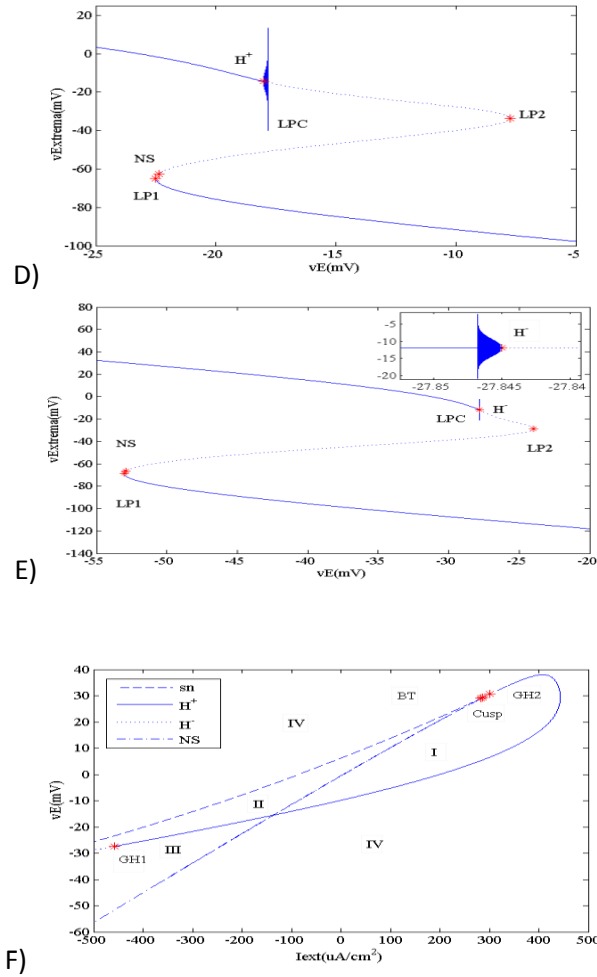
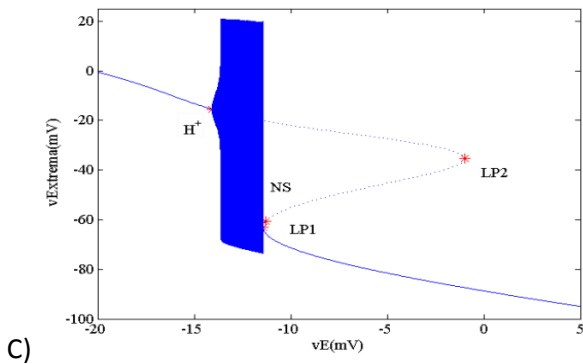
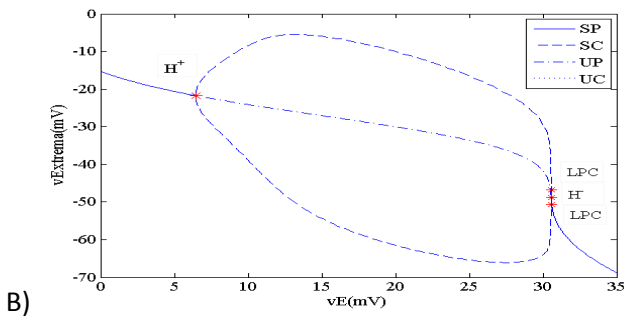
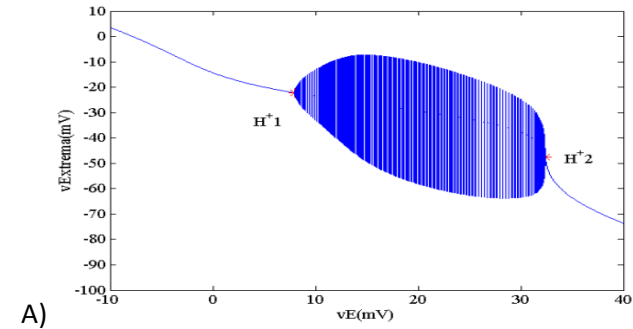


Fig.2. Single parameter bifurcation diagrams of vE for constant DC externally applied current I_{ext} A) 320, B) 300, C) -100, D) -200, and E) -470 $\mu A/cm^2$. F) 2BD of $(I_{ext}-vE)$ plane. The supercritical Hopf, subcritical Hopf, LPC, Neutral saddle, and limit point bifurcation points and curves are labeled as H^+ , H^- , LPC, NS, and sn (LP), respectively. In F), the points BT, Cusp, and GH represent Bogdanov-Takens, Cusp, and generalized Hopf bifurcations, respectively. In the single parameter bifurcation diagrams, except for B, solid and dotted curves and colored regions show stable point, unstable point, and limit cycles, respectively; moreover, in the diagram B SP, UP, SC, and UC curves represent stable equilibrium point, unstable equilibrium point, and the maximum and minimum of stable and unstable periodic orbits, respectively.

After the point LP2, the system has one stable equilibrium point. For $I_{ext}=-200 \mu A/cm^2$, Hopf bifurcation H^+ occurs between the points LP1 and LP2. In the region between the points LP1 and H^+ , two of the three equilibrium points are stable (Hysteresis or bistability of the equilibrium points). In a narrow region between points H^+ and LPC as shown in the Fig.2 (D), one of the three equilibrium points and a periodic orbit are stable (bistability of the equilibrium point and the periodic orbit). Note that, this is qualitatively different from the previous bistability. For $I_{ext}=-470 \mu A/cm^2$, Hopf bifurcation H^- occurs between the

points LP1 and LP2. Further, in the region between the points LP1 and LPC, two of the three equilibrium points are stable. Also, in a very narrow region between LPC and H^- two stable attractors (two stable equilibrium points) and one unstable point coexist with an unstable periodic orbit; moreover, the Fig.2 (F) is the 2BD of $(I_{ext}-vE)$ plane for $I_{Na,p}+I_K$ model.

The abscissa and ordinate are I_{ext} and vE , respectively. Four types of bifurcation curves are displayed. The solid, dotted, and dash-dotted curves represent supercritical Hopf, subcritical Hopf and neutral saddle node bifurcations. The V-shaped dashed curve is an LP (sn). Also, the subcritical Hopf bifurcation curve is terminated by the BT point on the lower right branch of the sn curve. On the Hopf bifurcation curves H^+ and H^- , there are two GH points. In region I, the periodic orbit is the unique stable steady state and an unstable equilibrium point exists within it. The asymptotic dynamics of the modified model $I_{Na,p}+I_K$ is the periodic oscillation. In region II and III, inside the V-shaped sn curve, the model $I_{Na,p}+I_K$ has three equilibrium points. In II, one of the three equilibrium points is stable. However, in III two of the three equilibrium points is stable (bistability of the equilibrium points). In region II, in the narrow region between the curves H^+ and LPC (the curve LPC has been not presented in the Fig.2 (D)), a few thousandth of millivolt above the curve H^+ , one of the three equilibrium points and a periodic orbit are stable (bistability of the equilibrium point and the periodic orbit). In region IV, the equilibrium point is the unique stable steady state, and the $I_{Na,p}+I_K$ behaves as an excitable membrane. Generally, there are two subtypes of excitability in IV. In one type, the membrane potential returns to its steady state directly after an excitation. In the other subtype, it shows damping oscillations after an excitation.

As regards, the single parameter bifurcation diagrams for $I_{Na,p}+I_K$ model are similar to the single parameter bifurcations of other models, only, the general two parameter bifurcation diagrams will be represented at $(I_{ext}-vE)$ plane in the next models.

3.2. $I_{Na,t}$ model

Fig.3 shows a bifurcation diagram of equilibrium points and limit cycles for $I_{Na,t}$ model in the $(I_{ext}-vE)$ plane. In I, the equilibrium point is the unique stable steady state and the $I_{Na,t}$ behaves as an excitable membrane. In II, the periodic orbit is the unique stable steady state and an unstable equilibrium point exists within it. Also, In III and IV, the $I_{Na,t}$ has three equilibrium points. In III, one of the them is stable. However, In IV three unstable equilibrium points coexist with one stable periodic orbit.

The LPC curve, is originated from the GH point, is located a few thousandth of millivolt above the curve H^- . Therefore,

in the narrow region between the curves H^- and LPC in region I, two limit cycles (one of them stable and another unstable) and stable equilibrium point coexist. While in the very narrow region between the curves H^- and LPC in region III, there are two periodic orbits (one of them is stable and another is unstable) and three equilibrium points (only, one equilibrium point is stable). Therefore, in this region, bistability of the equilibrium point and one periodic orbit occur.

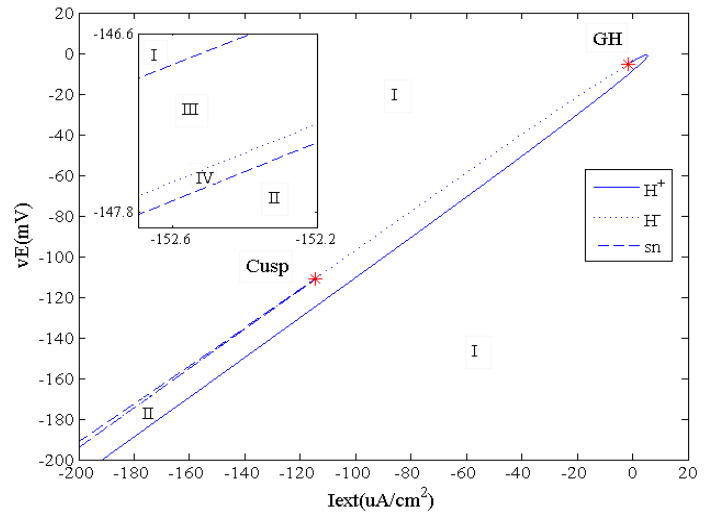


Fig.3. 2BD of $(I_{ext}-vE)$ plane for $I_{Na,t}$ model. The supercritical Hopf, subcritical Hopf and limit point bifurcation curves are labeled as H^+ , H^- and sn (LP), respectively. The points Cusp and GH represent Cusp, and generalized Hopf bifurcations, respectively.

3.3. $I_{Na,p}+I_h$ model

Fig.4 (A) shows the bifurcation diagram of the modified $I_{Na,p}+I_h$ model for positive injected DC currents. In region I, inside the V-shaped sn curve, there are three equilibrium point. Two of the them are stable (bistability of the equilibrium points). In II, outside the V-shaped sn, the equilibrium point is the unique stable steady state, and the $I_{Na,p}+I_h$ behave as an excitable membrane. Generally, there are two subtypes of excitability in I. In one type, the membrane potential returns to its steady state directly after an excitation. In another, it will respond as damping oscillations after an excitation.

In Fig.4 (B), the 2BD of modified $I_{Na,p}+I_h$ model for negative injected DC currents is indicated. In region III, the periodic orbit is the unique stable steady state and an unstable equilibrium point exist within it. The asymptotic dynamics of the $I_{Na,p}+I_h$ model is the periodic oscillation. In IV, there are three equilibrium points. One of the three equilibrium points is stable. In V, three unstable equilibrium points coexist with one stable periodic orbit. In the narrow regions between the curves H^- and LPC (the curve LPC has been not presented in the Fig.4 (B)), a few thousandth of millivolt above the curve H^- in II and a few thousandth of millivolt under the curve H^- in IV, two periodic orbit (one of the them stable and another unstable) coexist with one

stable equilibrium point (bistability of the equilibrium point and the periodic orbit).

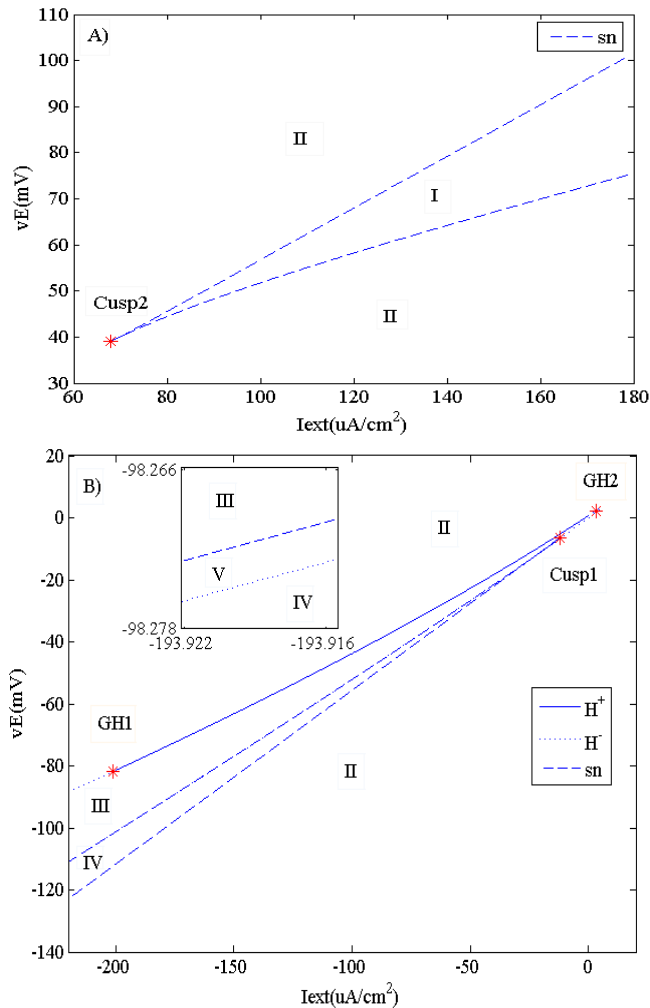


Fig.4. 2BDs of (I_{ext} - vE) plane for $I_{Na,p}+I_h$ model, A) positive injected DC currents, B) negative injected DC currents. The supercritical Hopf, subcritical Hopf and limit point bifurcation curves are labeled as H^+ , H^- and sn (LP), respectively. The points Cusp and GH represent Cusp, and generalized Hopf bifurcations, respectively.

3.4. I_h+I_{Kir} model

Fig.5 shows the loci in the plane of two parameters I_{ext} and vE , where a specific bifurcation occurs. In Figures 5(A) and 5(B), curves Hopf and LP (sn) are shown separately. In region I, there are three equilibrium points. Two of the three equilibrium points are stable (bistability of the equilibrium points). In II, the equilibrium point is the unique stable steady state. In Fig.5(C) it is difficult to distinguish curves Hopf (supercritical and subcritical) and sn and apparently there no stable periodic orbits. However, there is a very narrow region bounded between them where stable periodic orbits exist, although it is invisible at this scale.

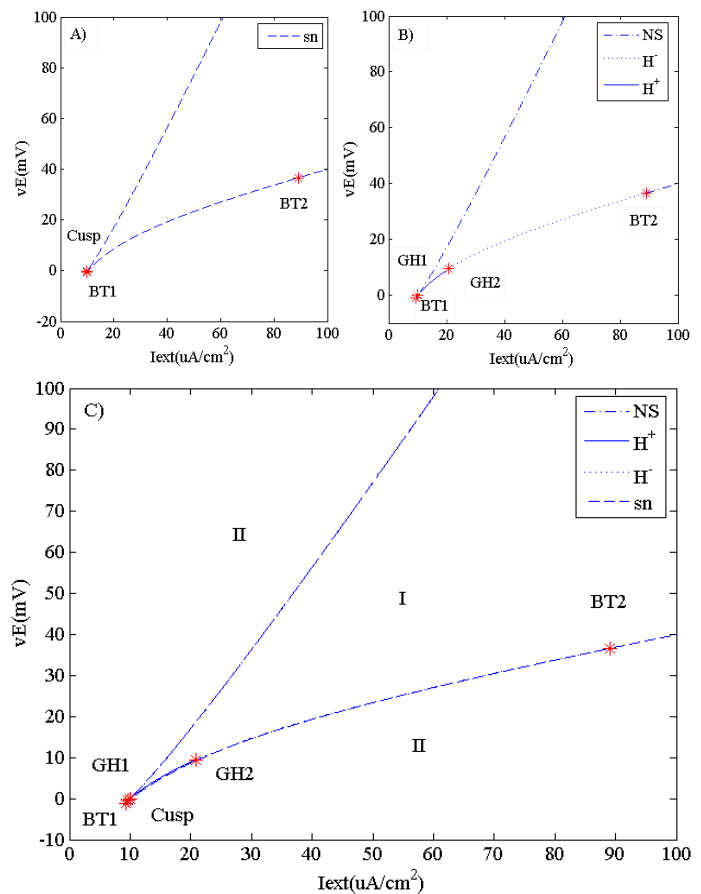


Fig.5. 2BDs of (I_{ext} - vE) plane for I_h+I_{Kir} model, A and B shows Hopf and sn curves separately. The supercritical Hopf, subcritical Hopf, neutral saddle and limit point bifurcation curves are labeled as H^+ , H^- , NS and sn (LP), respectively. The points Cusp, BT and GH represent Cusp, Bagdanov Takens and generalized Hopf bifurcations, respectively.

3.5. I_K+I_{Kir} model

Fig.6 shows the bifurcation diagram of the modified I_K+I_{Kir} model. In I, the equilibrium point is the unique stable steady stat, and I_K+I_{Kir} behave as an excitable membrane. However, similar to previous models, there are two subtypes of excitability in I. In II, the I_K+I_{Kir} have three equilibrium points. Two of the them are stable (bistability of the equilibrium points). In III, the periodic orbit is the unique stable steady stat. In the phase portrait of the system, an unstable equilibrium point is located inside the periodic orbit. In region IV, the I_K+I_{Kir} have three equilibrium points. However, two of the three equilibrium points are unstable. In V (Fig. 6(B)), the I_K+I_{Kir} have five equilibrium points. Two of the five equilibrium points are stable (bistability of the equilibrium points). In region I, in the narrow region between the curves H^- and LPC (the curve LPC has been not presented in the Fig.6 for the sake of clarity), a few thousandth of millivolt above the curve H^- , one stable equilibrium point coexist with two periodic orbits(one stable and another unstable). Therefore, bistability of the equilibrium point and the periodic orbit occurs.

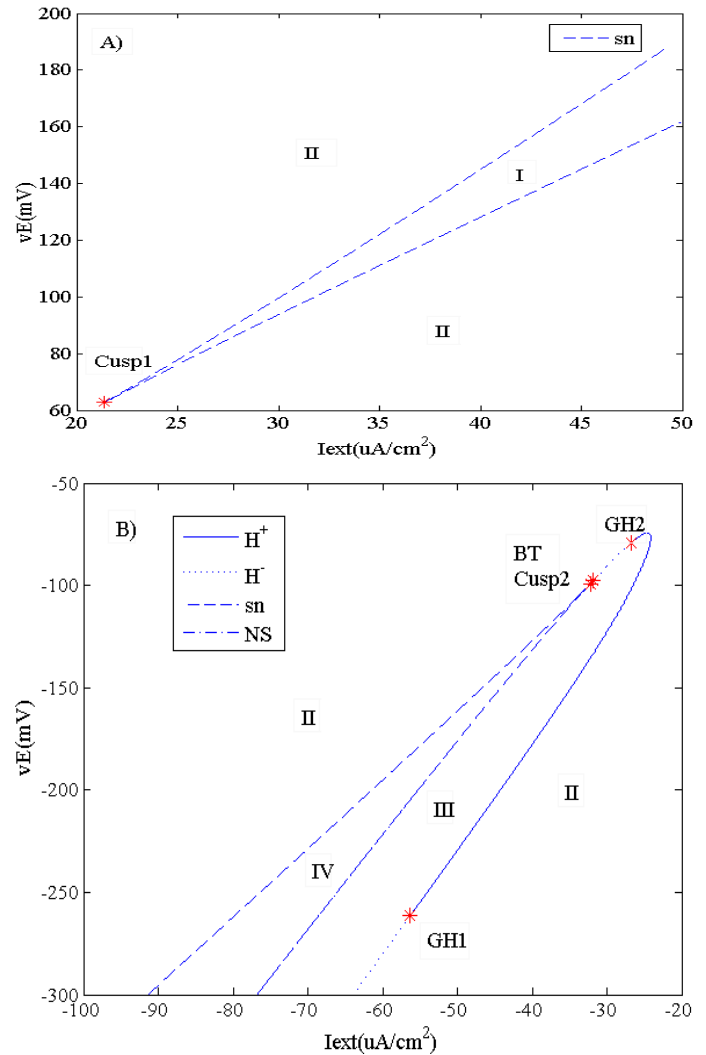
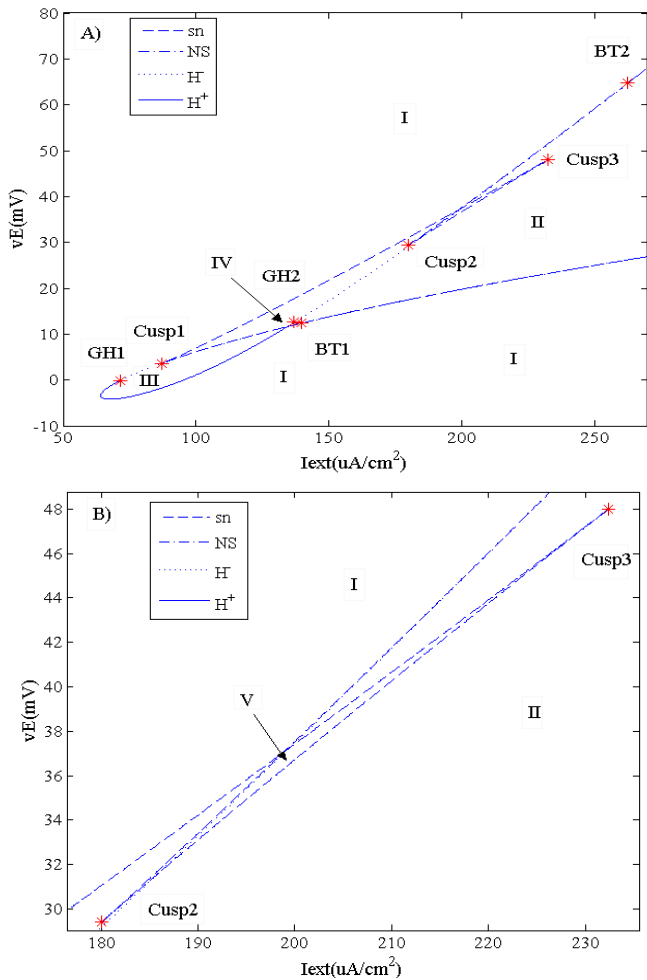


Fig.6. 2BDs of $(I_{ext}-vE)$ plane for I_K+I_{Kir} model, The supercritical Hopf, subcritical Hopf, neutral saddle and limit point bifurcation curves are labeled as H^+ , H^- , NS and sn (LP), respectively. The points Cusp, BT and GH represent Cusp, Bagdanov Takens and generalized Hopf bifurcations, respectively.

3-6 I_A model

Fig.7 shows a bifurcation diagram of equilibrium points and limit cycles for I_A model in the $(I_{ext}-vE)$ plane. In region I, there are three equilibrium points. Two of the three equilibrium points are stable (bistability of the equilibrium points). In II, the equilibrium point is the unique stable steady state and the I_A behaves as an excitable membrane. In III, the periodic orbit is the unique stable steady stat. In the phase portrait of the system, an unstable equilibrium point is located inside the periodic orbit. In IV, inside the V-shaped sn curve, there are three equilibrium point. Two of the them are unstable. In region II, in the narrow region between the curves H^- and LPC (the curve LPC has not been presented in the Fig.7 for the sake of clarity), a few thousandth of millivolt above or under the curve H^- , one stable equilibrium point coexist with two periodic orbits (one stable and another unstable). Thus, bistability of the equilibrium point and the periodic orbit occurs.

applied DC current) as the abscissa and induced voltage component as the ordinate. In each diagram, the

Fig.7. 2BDs of $(I_{ext}-vE)$ plane for I_A model, A) positive injected DC currents, B) negative injected DC currents. The supercritical Hopf, subcritical Hopf, neutral saddle and limit point bifurcation curves are labeled as H^+ , H^- , NS and sn (LP), respectively. The points Cusp, BT and GH represent Cusp, Bagdanov Takens and generalized Hopf bifurcations, respectively.

In all models, the regions, in which limit cycles (one is stable and another is unstable) and a stable equilibrium point coexist, are located at a few thousandth of a millivolt of the Hopf bifurcation curve. These regions are hardly detectable and not shown in 2BDs. According to the 2BDs, unlike Hodgkin-Huxley model that is affected by ELF electric fields [8], the minimal models, are always monostable or bistable when are affected by the mentioned fields. Also, the minimal models, $I_{Na,p}+I_h$ and I_h+I_{Kir} , have maximum and minimum dynamic variations, respectively. Note that, the $I_{Na,p}+I_h$ and I_h+I_{Kir} have 7 and 3 different dynamical regions, respectively.

4. DISCUSSION

We have investigated bifurcations observed in the minimal cell models. Results are summarized in various two parameter bifurcation diagrams with I_{ext} (externally

Global analysis of the bifurcation structure suggested that generation of these regions is associated with GH and LPC bifurcations. Also, results of this study shows that due to

existence of only an amplifying gating variable and one resonant gating variable in structure of minimal models, multi-stabilities of higher order than two do not occur.

5. REFERENCES:

1. Kocherginsky Nikolai. Voltage sensitive ion channels, acidic lipids and Hodgkin-Hoxley equations new ideas 55 years later. *Journal of membrane science*. 2008; 328:58-74.
2. Hidekazu Fukai, Shinji Doi, Taishin Nomura. Hopf bifurcations in multiple-parameter space of the Hodgkin-Huxley equations I. Global organization of h bistable periodic solutions. *Biol Cybern*. 2000; 82: 215-222.
3. J. Guckenheimer, I. S. Labouriau. Bifurcation of the Hodgkin and Hoxley equations: A new twist. *Bulletin of Mathematical Biology*. 1993; 55:937-952.
4. M. Morel, Cachan, F. Takens, Groningen, B. Teissier. Tutorials in Mathematical Biosciences I. *Springer-Verlag Berlin Heidelberg*. 2005.
5. Eugene M. Izhikevich. Dynamical Systems in Neuroscience: The Geometry of Excitability and Bursting. *Springer-Verlag*. 2007.
6. Shinji Doi, Shuhei Nabetani, Sadatoshi Kumagai. Complex nonlinear dynamics of the Hodgkin-Hoxley equations induced by time scale changes. *Biol Cybern*. 2001; 85:51-64.
7. Stephen T. Kee, Julie Gehl, Edward W. Lee. Clinical Aspects of Electroporation: The cell in the electric field. 1st ed. *Springer*. 2011; 1:19–29.
8. Che. Yanqiu and J. Wang. Bifurcations in the Hodgkin–Huxley model exposed to DC electric fields. *Neurocomputing*. 2012; 81:41–48.
9. T.Kotnik, F. Bobanovic, D. Miklavcic. Sensitivity of transmembrane voltage induced by applied electric fields-a theoretical analysis. *Bioelectrochemistry and Bioenergetics*. 1997; 43:285-291.
10. Cellular open Resource, <http://cor.physiol.ox.ac.uk>.
11. A. Dhooge, W. Govaerts, u. A. Kuznetsov, "MATCONT: A MATLAB Package for Numerical Bifurcation Analysis of ODEs", *ACM Transactions on Mathematical Software*.2003; 29:141-16.

Conflict of Interest: None Declared

Cite this article as:

A. Naghilou, S.H.Sabzpoushan. Evaluation of ELF Electric Fields Effects on Bifurcation Phenomenon of Spaced-Clamped Conductance-Based Minimal Cell Models. *Asian Journal of Biomedical and Pharmaceutical Sciences*, 2013, 3: (20), 8-16.